CHEMMEDCHEM

DOI: 10.1002/cmdc.200800424

Surface-Functionalized Ultrasmall Superparamagnetic Nanoparticles as Magnetic Delivery Vectors for Camptothecin

Feride Cengelli,[a] Justyna A. Grzyb,[b] Auxia Montoro,[a] Heinrich Hofmann,[c] Stephen Hanessian,*[b] and Lucienne Juillerat-Jeanneret*[a]

The linking of therapeutic drugs to ultrasmall superparamagnetic iron oxide nanoparticles (USPIOs) allowing intracellular release of the active drug via cell-specific mechanisms would achieve tumor-selective magnetically-enhanced drug delivery. To validate this concept, we covalently attached the anticancer drug camptothecin (CPT) to biocompatible USPIOs (iron oxide core, 9–10 nm; hydrodynamic diameter, 52 nm) coated with polyvinylalcohol/polyvinylamine (PVA/aminoPVA). A bifunctional, end-differentiated dicarboxylic acid linker allowed the attachment of CPT to the aminoPVA as a biologically labile ester substrate for cellular esterases at one end, and as an amide at the other end. These CPT–USPIO conjugates exhibited antiproliferative activity in vitro against human melanoma cells. The intracellular localization of CPT–USPIOs was confirmed by transmission electron microscopy (iron oxide core), suggesting localization in lipid vesicles, and by fluorescence microscopy (CPT). An external static magnetic field applied during exposure increased melanoma cell uptake of the CPT–USPIOs.

Introduction

The vast majority of clinically used therapies for cancer capitalize on differences in the rate of cell replication between tumoral and nontumoral cells. In general, therapeutic agents distribute through the whole body, which results in general toxicity, a suboptimal concentration of the therapeutic agent in the tumor and poor therapeutic response.[1] Therefore, in order to improve cancer treatments, it is necessary to optimize the delivery and biodistribution of drugs to diseased organs, tissues or cells, by devising therapeutic formulations that allow increased localized concentrations of the therapeutic agents in the target tissues for longer time periods.

Most solid tumors possess defective vascular architecture, increased vascular permeability and leaky vessels. The enhanced permeability and retention (EPR) effect allows the passage and distribution of micro/nanoparticulate devices, offering therapeutic windows for the delivery of drug substances. To take advantage of these defects in tumor vasculature, drugs have been linked to macromolecular structures, polymers or micro/nanocarriers as vectors.[2–7] However, the retention time in diseased tissue is generally low. Therefore, it is imperative that nanoparticulate drug carriers are capable of residing in defined locations for longer periods of time, while releasing therapeutic agents in the appropriate environment at the requisite rate and dose.

Sustained and elevated tissue concentrations were achieved with intra-articularly administered ultrasmall superparamagnetic iron oxide nanoparticles (USPIOs) when an external magnet was applied on the joint.[8] Colloidal dispersions of USPIOs add a unique function to nanoparticles due to their magnetic properties.[9–12] A strategically interesting way to achieve site-selective delivery is by chemical attachment of therapeutic agents to USPIOs via a cell-specific labile linkage, and steering the drug–USPIO assembly to specific diseased areas in the body under the influence of an external magnetic field. This implies that the drug–nanoparticle assembly must be internalized by cells, that this uptake be enhanced by an external magnetic field, and subsequently, that the drug be released intracellularly to exert its expected therapeutic effects.

The design, preparation and evaluation of magnetic nanoparticles displaying drugs at their surface are only in their early phase of development.[7] Creating the toolbox of anticancer molecules that can be hierarchically assembled into an ordered, spatially and chemically defined architecture at the surface of magnetically active nanoparticles is a major synthetic challenge. The attachment of drugs to biocompatible USPIOs through ester linkages that can be cleaved by esterases once inside a cancer cell would offer a possible solution to selective drug delivery.[13] The potential of drug delivery based on magnetically activated nanoparticles has been evaluated in vivo

[a] F. Cengelli,[+] A. Montoro, Dr. L. Juillerat-Jeanneret
Centre Hospitalier Universitaire Vaudois and University of Lausanne
University Institute of Pathology
Rue du Bugnon 25, CH-1011 Lausanne (Switzerland)
Fax: (+41) 21-314-7115
E-mail: lucienne.juillerat@chuv.ch

[b] Dr. J. A. Grzyb,[+] Prof. Dr. S. Hanessian
Department of Chemistry, University of Montreal
P.O. Box 6128, Station Centre-ville, Montreal, QC, H3C 3J7 (Canada)
Fax: (+514) 343-5728
E-mail: stephen.hanessian@umontreal.ca

[c] Prof. Dr. H. Hofmann
Powder Technology Laboratory
Institute of Materials, Swiss Federal Institute of Technology
EPFL, MX-Ecublens, 1015 Lausanne (Switzerland)

[+] These authors contributed equally to this work

with significant advantages, including the possibility of achieving targeted delivery and decreased off-target effects.[14–20] For example, the covalent attachment of methotrexate at the surface of USPIOs and its release in vivo by lysosomal proteases has led to a study of its therapeutic potential.[21–23] However, to the best of our knowledge, the attachment and delivery of ester-linked anticancer agents to USPIOs has not been exploited successfully.

The plant alkaloid camptothecin (CPT) and its analogues are specific inhibitors of the nuclear DNA topoisomerase I,[24,25] and are active as cytostatic drugs against many solid tumors, including melanoma.[26] To improve the low solubility of CPT, chemical modifications, conjugation to polymers, intercalation into liposomes, solubilization in microemulsions, and entrapment in microspheres and micellar colloidal particles have been studied.[27,28]

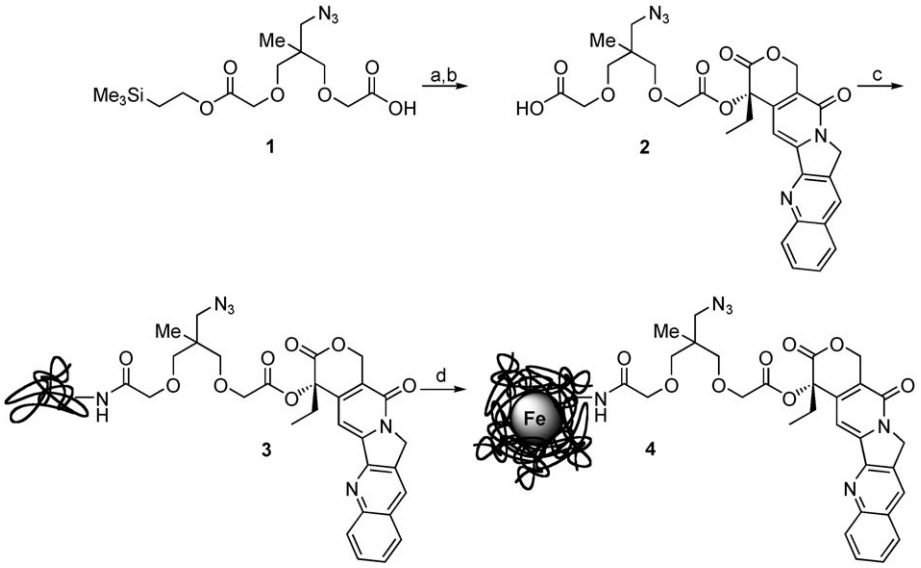

Scheme 1. *Reagents and conditions*: a) camptothecin, EDC, DMAP, CH_2Cl_2, RT, o/n; b) TFA/CH_2Cl_2 (1:1), RT, 40 min; c) EDC, HOBt, aminoPVA, DMF/H_2O, RT, 1 d; d) ferrofluid.

We have previously reported the preparation and characterization of various USPIOs coated with polyvinylalcohol/polyvinylamine mixtures, which were internalized by nonphagocytic human tumor cells.[29–31] Bifunctional linkers to which the anticancer drugs doxorubicin or 5-fluorouridine were attached by either amide or ester linkages were also previously reported.[32] In the present work, we studied the efficacy of the potent anticancer agent CPT attached as an ester to an amide-linked bifunctional spacer to aminoPVA polymers containing USPIOs. Herein, we report the uptake of such CPT–USPIO conjugates, their effect on cells, and the potential utility of an external magnet to enhance their uptake in human melanoma cancer cells.

Results and Discussion

Chemistry

Firstly, CPT was covalently attached via its hydroxyl group at position 20 to the aminoPVA polymer through an end-differentiated azido dicarboxylic acid linker **1**.[32] This linker contains two carboxylic acid groups, which were used for attachment of CPT at one end, and coupling to the aminoPVA at the other, prior to addition of the ferrofluid to formulate the final CPT–USPIOs **4** (Scheme 1). Esterification of the tertiary alcohol of CPT was done in the presence of EDC and DMAP. Cleavage of the Me_3Si ethyl ester gave the carboxylic acid **2**, which was coupled with aminoPVA in aqueous DMF to give the CPT–linker conjugate **3**. The product was purified by dialysis and residual free drug was removed from a lyophilized white solid by repeated trituration with CH_2Cl_2. In order to quantify the amount of drug linked to the polymer, an azide group was incorporated in the linker to calculate the ratio of the area under the azide peak at 2100 cm^{-1} to that of a reference peak in the aminoPVA at 1100 cm^{-1} in the IR spectra of coupled products, as previously described.[32] This method demonstrated that 24% of the amino groups of the aminoPVA were substituted by CPT.

Preparation and characterization of CPT–USPIOs 4

Superparamagnetic iron oxide nanoparticles (9 nm iron oxide core, ferrofluid) were prepared by alkaline coprecipitation of ferric and ferrous salts, as previously described.[29–31] The CPT–USPIO conjugate **4** was prepared by adding the ferrofluid to mixtures of PVA/aminoPVA/CPT–linker–aminoPVA **3** to obtain homogeneous amber-brown colored solutions. We previously showed that USPIO conjugates coated with PVA/aminoPVA at a ratio of 45:1 (*w*/*w*) and a polymer/iron ratio of 10:1 (*w*/*w*), with a defined positivity, are biocompatible and efficiently taken up by cells.[29–31] Therefore, a constant ratio of total polymer to iron of 10 was maintained, and the positively charged surface of CPT–USPIO conjugate **4** was maintained by compensating for the loss of the amino groups of the aminoPVA (due to drug substitution) by increasing the ratio of aminoPVA to PVA during coating of the ferrofluid (Table 1).

The hydrodynamic size and surface charge determined by photon correlation spectroscopy (PCS), electrophoretic mobilities (charge/size ratio) and zeta (ζ) potential of the CPT–USPIO conjugate **4** and the model aminoPVA-USPIOs[30] were very comparable (Table 2). The physicochemical characteristics of CPT–USPIO conjugate **4** were consistent with their expected composition. CPT–USPIO conjugate **4** had comparable particle size and size distribution to aminoPVA-USPIOs as measured by PCS, but slightly lower charge positivity.

Table 1. Quantitative composition determination of the CPT–USPIOs **4**.[a]

	CPT–aminoPVA [%, *w*/*v*]	PVA [%, *w*/*v*]	aminoPVA [%, *w*/*v*]	Iron [%, *w*/*v*]	CPT [μM]
CPT–USPIOs **4**	0.8	37.5	0.2	3.8	357

[a] The substitution by CPT of the amino groups of the aminoPVA represented 24% of the total number of amino groups.

Table 2. Size, amino group concentration, electrophoretic mobility and ζ-potential of the amino-USPIOs and CPT–USPIOs **4**.

	Size[a] [nm]	Free amino groups[b] [mM]	Mobility [10^{-8} $ms^{-1}V^{-1}m$]	ζ-potential [mV]
aminoPVA-USPIOs	56.4 ± 4.1	1.59	1.33 ± 0.04	17.0 ± 0.5
CPT–USPIOs **4**	52.1 ± 7.7	1.49	0.42 ± 0.13	6.4 ± 1.3

[a] Nanoparticle hydrodynamic diameter. [b] Residual free amino groups on the aminoPVA were calculated from the known number (2.5% N, *w*/*w*) of amino groups in unfunctionalized aminoPVA and the number of bound CPT per aminoPVA.

the observed effects. AminoPVA-USPIOs had no effect on DNA synthesis in melanoma cells (results not shown). In order to determine whether the bulky structure of CPT–USPIO conjugate **4** could be a substrate for melanoma cell esterases, it was exposed to human Me300 melanoma cell extracts and the specific CPT fluorescence, as well as iron and PVA, were evaluated by gel-filtration (Figure 1b). The results clearly demonstrated an important increase in free CPT fluorescence in the low molecular weight fractions, providing evidence that the ester bond linking CPT to the USPIOs via the linker was accessible to cellular esterases of human melanoma cells, and that these esterases have the potential to release the drug from the nanoparticle–linker carrier, despite the bulky structure of the conjugate.

Cellular assays

The human Me300 melanoma cells were selected from a panel of human cancer cells for their high uptake of aminoPVA-USPIO and CPT–USPIO. To evaluate the stability of the CPT–USPIO conjugate **4** at physiological pH, gel filtration was performed at pH 7, and the elution profile of iron and PVA was compared to the fluorescence associated with CPT (Figure 1). The CPT–USPIO conjugate **4** eluted as a major single high molecular weight fraction encompassing iron, PVA and CPT (Figure 1a). The gel filtration fractions were evaluated for biological activity and revealed that a peak corresponding to a major high molecular weight component, combining CPT, the PVA polymer and iron, corresponding to CPT–USPIO conjugate **4**, efficiently decreased DNA synthesis in melanoma cells (Figure 1a, insert).

A minor, iron-negative and PVA-negative, lower molecular weight peak exhibited some efficacy in inhibiting DNA synthesis in melanoma cells (Figure 1a, insert), suggesting only minimal hydrolytic release of CPT from the carrier at this pH over time, which alone can not account for

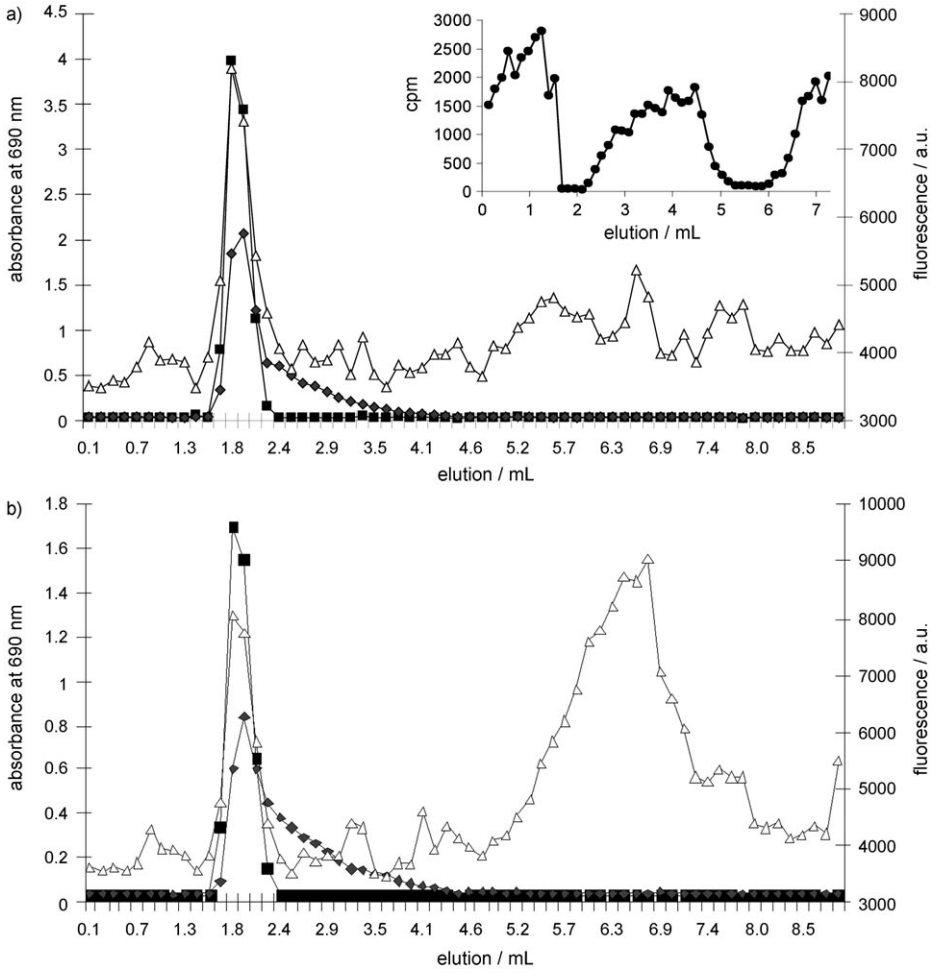

Figure 1. The CPT–USPIOs were gel filtrated on Sephadex G-75 in PBS at pH 7. Iron and PVA were quantified at 690 nm by Prussian blue and iodine reactions, respectively, and camptothecin (CPT) by fluorescence in H_2O at λ_{ex}/λ_{em} of 360/460 nm. a) Gel filtration of CPT–USPIOs **4**; Iron (■); PVA (◆); CPT (△). *Insert*: biological activity of the gel filtration fractions evaluated by inhibition of DNA synthesis in human Me300 melanoma cells (^{3}HT incorporation [cpm]) (●). b) Evaluation by gel filtration of the release of CPT from CPT–USPIOs **4** pre-incubated for 24 h at 37 °C with PBS extract of Me300 cells. Iron (■); PVA (◆); CPT (△).

The amount of CPT–USPIO conjugate **4** taken up by human Me300 melanoma cells after 16 h and 36 h as a function of the number of nanoparticles added was determined by the amount of cell-associated iron and cell-associated CPT fluorescence (Figure 2a and b, inserts) as compared with that of the previously described aminoPVA-USPIOs.[30] After 16 h, the uptake of aminoPVA-USPIOs and CPT–USPIO conjugate **4** was comparable (Figure 2a). However, after 36 h, uptake of cytotoxic conjugate **4** continued to increase in the still-surviving cells, whereas the uptake of noncytotoxic aminoPVA-USPIOs had ceased due to saturation (Figure 2b). Histological determination of cell-associated iron (Figure 2c) and CPT fluorescence (Figure 2d) showed incorporation of CPT–USPIO conjugate **4** in the melanoma cells. The intracellular localization of the iron oxide core of the conjugate **4** in cell organelles was further demonstrated by transmission electron microscopy (TEM) (Figure 2e). The appearance of the vesicles was suggestive of lipid vesicles. In order to confirm the localization of CPT–USPIO **4** in melanoma cells, histological staining for lipids (Figure 3a and b), TEM imaging (Figure 3c) and elemental analysis of USPIO containing granules (Figure 3d) were performed, strongly suggesting localization of CPT–USPIO in lipid vesicles.

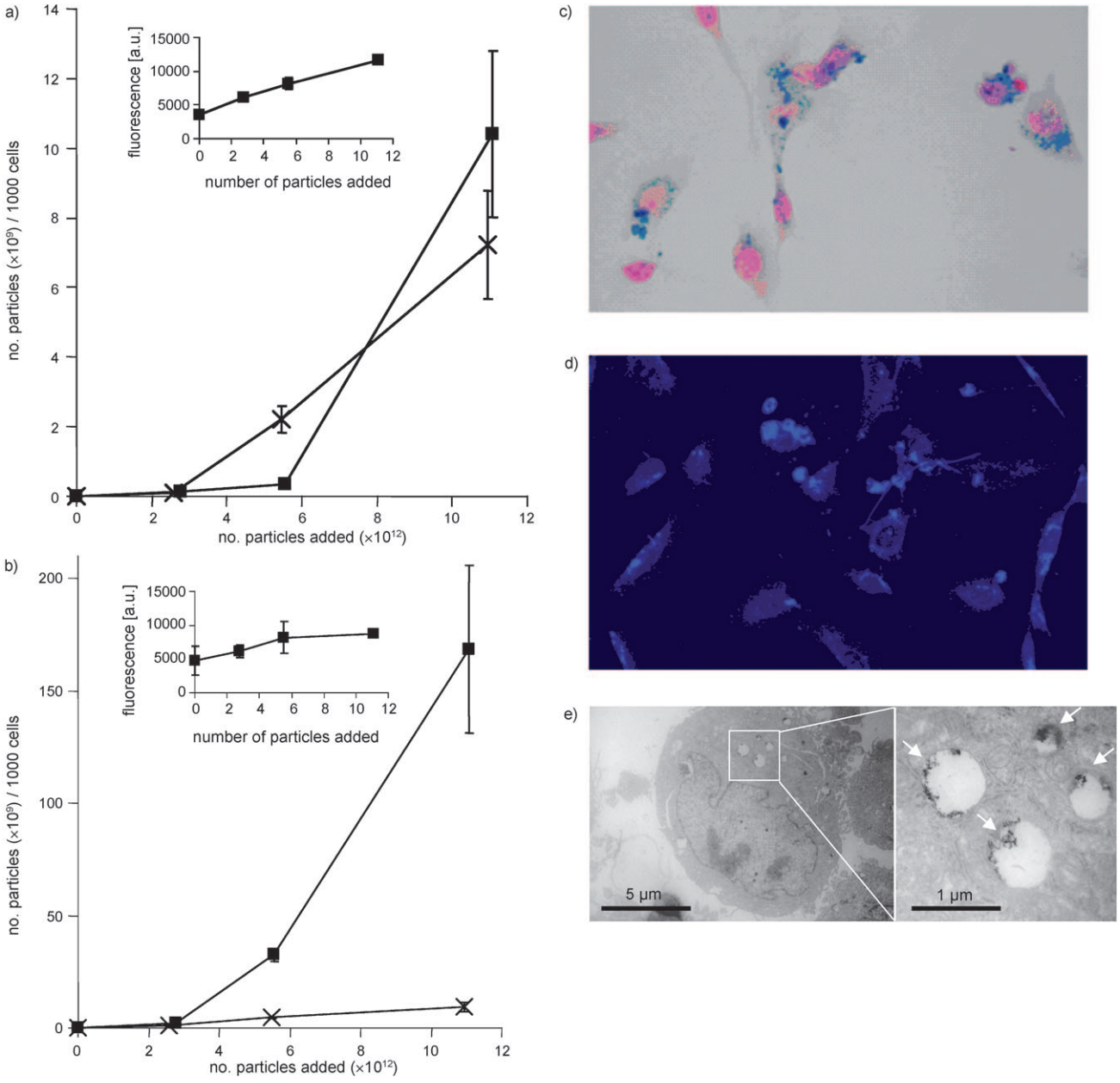

Figure 2. Human Me300 melanoma cells were exposed for a) 16 h or b) 36 h to increasing concentrations of the CPT–USPIOs **4** or aminoPVA-USPIOs and cell iron content was determined. CPT–USPIOs **4** (■); aminoPVA-USPIOs (×). The uptake by cells of CPT associated to the USPIOs was determined by its specific cell-associated fluorescence in the intact cell layer (■, inserts). The uptake of CPT–USPIOs (0.7 µM CPT in CPT–USPIOs, 8 µg Fe mL^{-1}) after 36 h was also examined in parallel cultures of Me300 cells grown on histological slides: c) histological Prussian blue reaction; d) CPT cell-associated characteristic fluorescence; and e) transmission electron microscopy (TEM) demonstrating the iron oxide core of the CPT–USPIOs in intracellular organelles (⁄).

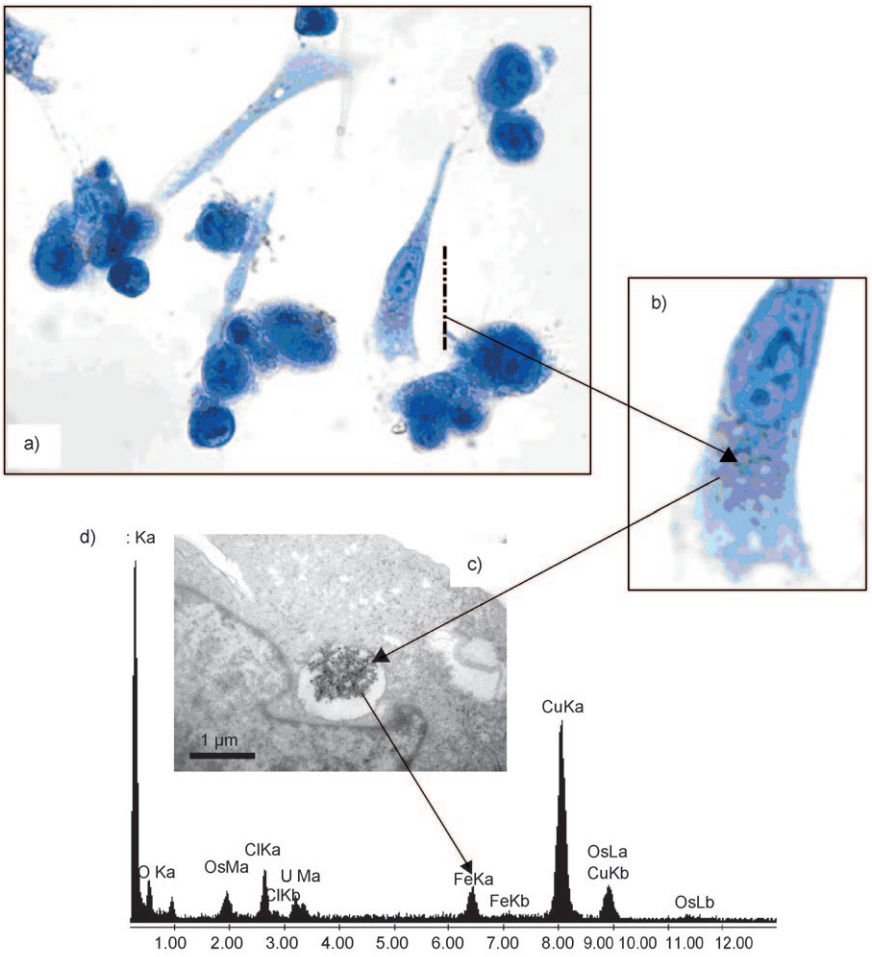

Figure 3. Human Me300 melanoma cells were exposed to CPT–USPIOs (8 μg Fe mL^{-1}, 0.7 μM CPT) for 36 h, and a) stained by Sudan for lipid visualization (brownish spots, see b) for magnification) or c) examined by TEM imaging. d) Elemental analysis of iron was also performed.

The effect of CPT–USPIO conjugate **4**, compared with free CPT, on the survival of human melanoma cells was evaluated using the Alamar Blue reaction and DNA synthesis (Figure 4). The effect of free CPT either on DNA synthesis or cell survival was already apparent after 16 h exposure (Figure 4a) and was enhanced after 36 h (Figure 4b). As expected for this type of anticancer agent, inhibition of DNA synthesis preceded decrease in cell survival, which was apparent only after 36 h of exposure (Figure 4b). The time dependency of antiproliferative activity of CPT–USPIO conjugate **4** was slower than that of free CPT.

Due to the superparamagnetic properties of USPIOs, we expected the local concentration at the cell surface and/or uptake by cells of CPT–USPIO conjugate **4**, compared to free CPT, to be enhanced by applying an external magnetic field. An experimental system was devised consisting of a 48-well plate whose wells were filled with round static magnets and inserted under a similar 48-well plate containing the human melanoma cells (Fig-

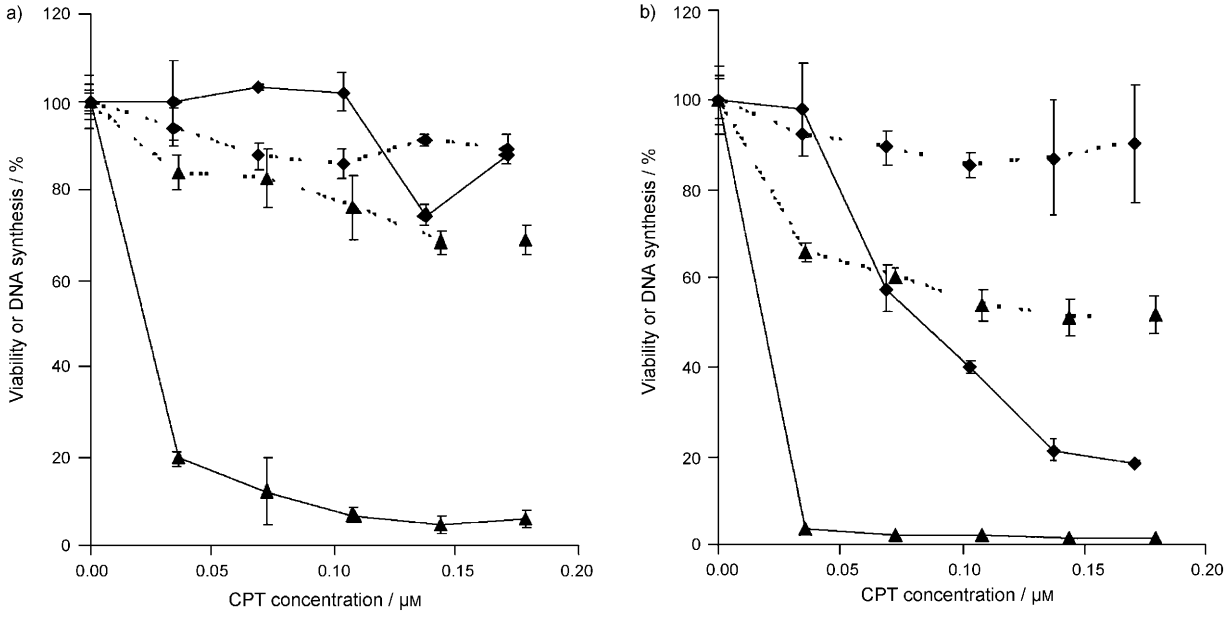

Figure 4. Human Me300 melanoma cells were exposed for a) 16 h or b) 36 h to increasing concentrations of CPT or the CPT–USPIOs **4** and either cell survival (Alamar Blue reduction, AlaB) or DNA synthesis ([^{3}H]-thymidine incorporation, 3HT) were determined. CPT–USPIOs **4** (AlaB) (◆, •••••); CPT–USPIOs **4** (3HT) (◆, ——); free CPT (AlaB) (▲, •••••); free CPT (3HT) (▲, ——).

ure 5a). The loss of the magnetic field as a function of the distance to the magnet was calculated (Figure 5b). Under the experimental conditions, the cell layer was exposed to a 265 mT magnetic field that decreased almost linearly to reach less

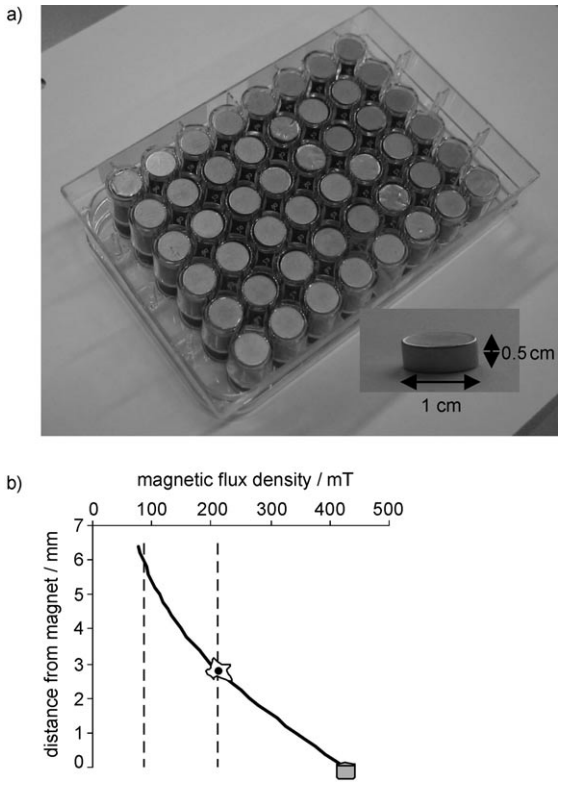

Figure 5. Experimental setting: magnetic flux density [mT] as a function of the distance to the magnet surface [mm]. Magnet (0 mm): 424 mT; cell layer (2.8 mm): 212 mT; upper level of the CPT–USPIOs solution in the culture wells (6 mm): 85 mT.

than 100 mT at the surface of the cell culture medium. The results clearly demonstrated that exposure to the magnetic field increased the binding of the conjugate **4** to human melanoma cells as measured by cell-associated iron (not shown) and CPT fluorescence (Figure 6a). Thus, the superparamagnetic properties of drug–USPIOs with an iron oxide core of ~10 nm increased cell-associated iron and drug content. However, whereas the magnetic field increased cell content of the conjugate **4**, the time-dependent antiproliferative effect of the conjugate was not increased (Figure 6b and c). This information strongly suggests that the limiting rate for antiproliferative efficacy is not the uptake of these drug–USPIOs by cells, but the release of the drug from its nanoparticulate carrier via an esterolytic step, and its diffusion out of the cell organelle(s) and into the cell nucleus.

Conclusions

In summary, a viable synthetic route to USPIOs containing a polymer, a linker and a covalently linked anticancer drug (CPT) have been examined in this study. We demonstrated that a hierarchical building of a covalent drug–USPIO assembly is possible, even for highly hydrophobic drugs like CPT. The uptake of the CPT–USPIOs by human melanoma cells resulted in decreased cell survival as estimated from the decrease in metabolic activity and DNA synthesis after long-term exposure. The exposure of the melanoma cell layer to a permanent static magnet increased the amount of cell-associated CPT–USPIOs in melanoma cells, suggesting that the same effect could be achieved in vivo. However, the rate-limiting step for therapeutic efficacy is the bioprocessing of these superparamagnetic vectors by cellular mechanisms. The cell uptake mechanisms, the accessibility of the conjugate to esterolytic enzymes for drug release, and the intracellular routing of these CPT–USPIO assemblies are of utmost importance and must be collectively considered for efficient drug delivery. Further studies in this fascinating area of magnetically-directed drug delivery are under active investigation and will be reported in due course.

Experimental Section

Chemistry

General

All commercially available reagents were used without further purification. All reactions were performed under nitrogen atmosphere. NMR (^{1}H, ^{13}C) spectra were recorded on Bruker ARX-400, AV-300 and AV-400 RG spectrometers. Low- and high-resolution mass spectra were recorded using electrospray technique. Optical rotations were recorded on a Perkin–Elmer Model 343 polarimeter in a 1 dm cell at room temperature. Analytical TLC was performed on precoated silica gel plates. Flash column chromatography was performed using (40–63 μm) silica gel. IR was measured on a Perkin–Elmer Spectrum One FT-IR spectrometer. IR spectra of organic compounds were taken as films, while of polymer mixtures were taken after an aqueous polymer sample was mixed with KBr and lyophilized to give a fine powder that was pressed into a disk.

Nanoparticle synthesis

[2-Azidomethyl-3-(4-ethyl-3,13-dioxo-3,4,12,13-tetrahydro-1*H*-2-oxa-6,12a-diaza-dibenzo[*b,h*]fluoren-4-yloxycarbonylmethoxy)-2-methyl-propoxy]-acetic acid (2): The synthesis and characterization of **1** has been previously described.[32] A solution of **1** (0.093 g, 0.26 mmol) in CH_2Cl_2 (3.5 mL) was treated with camptothecin (0.060 g, 0.17 mmol), DMAP (0.015 g, 0.12 mmol) and EDC (0.132 g, 0.69 mmol) and the reaction mixture was stirred overnight at RT. The solvent was evaporated and the residue was purified by column chromatography ($CHCl_3$/MeOH, 100:0→99:1) to give the coupled product as a yellow solid (0.109 g, 92%); mp 112–114 °C; ^{1}H NMR (300 MHz, $CDCl_3$): δ = 8.40 (1H, s), 8.22 (1H, d, J = 8.5 Hz), 7.94 (1H, d, J = 8.1 Hz), 7.87–7.81 (1H, m), 7.70–7.65 (1H, m), 7.21 (1H, d, J = 1.3 Hz), 5.67 (1H, d, J = 17.2 Hz), 5.39 (1H, d, J = 17.2 Hz), 5.29 (2H, s), 4.34–4.16 (4H, m), 4.10–3.98 (2H, m), 3.46–3.30 (6H, m), 2.36–2.11 (2H, m), 1.04–0.94 (8H, m), 0.04–0.01 ppm (9H, m); ^{13}C NMR (75 MHz, $CDCl_3$): δ = 170.5, 169.5, 167.3, 157.3, 152.3, 148.9, 146.5, 145.5, 131.3, 130.8, 129.6, 128.5, 128.3, 128.2, 128.1, 120.3, 95.9, 76.4, 74.5, 74.1, 68.8, 68.4, 67.2, 63.1, 55.2, 50.0, 41.1, 31.9, 17.8, 17.4, 7.6, −1.5 ppm; IR (neat/NaCl): $\tilde{\nu}$ = 2950, 2102, 1755, 1672, 1623, 1128 cm^{-1}; LRMS (ESI): m/z [MH]$^+$ 692.

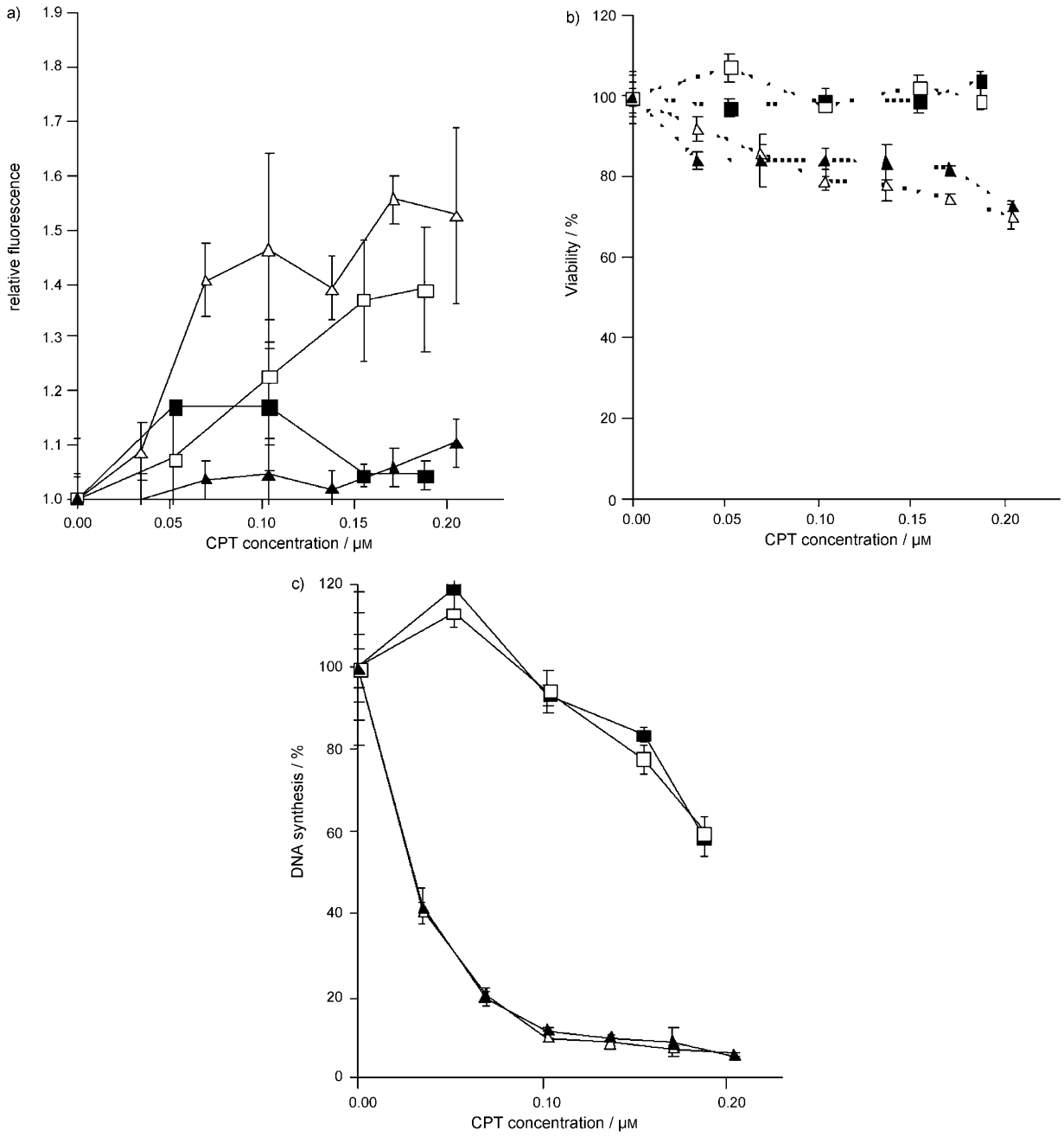

Figure 6. a) Human Me300 melanoma cells were grown in 48 well-plates and exposed for 16 h or 36 h to CPT–USPIOs (21 μg Fe mL^{-1}) either in the absence of or on a permanent static magnet, then CPT uptake by cells was quantified by fluorescence at 360/460 nm. (■): 16 h without magnet; (□): 16 h with magnet; (▲): 36 h without magnet; (△): 16 h with magnet, followed by 20 h without magnet. After exposure with or without a permanent static magnet of human Me300 melanoma cells to CPT–USPIOs **4**, b) cell survival was ascertained by Alamar Blue staining (•••••) or c) DNA synthesis by melanoma cells was determined by [^{3}H]-thymidine incorporation (——) performed during the 2 last hours. (■): 16 h without magnet; (□): 16 h with magnet; (▲): 36 h without magnet; (△): 16 h with magnet, followed by 20 h without magnet.

The ester (0.109 g, 0.16 mmol) was dissolved in TFA/CH_2Cl_2 (1:1, 6 mL) and stirred at RT for 40 min. The solvent was removed in vacuo and traces of TFA were removed by co-evaporating with MeOH. Column chromatography (CH_2Cl_2/MeOH, 9:1) gave the desired product **2** as an off-white solid (0.082 g, 88%). *Warning; $CHCl_3$ or $CDCl_3$ may cause decomposition of this compound*; ^{1}H NMR (400 MHz, [D_6]DMSO): $\delta = 8.66$ (1H, s), 8.15–8.08 (2H, m), 7.85 (1H, t, $J = 7.7$ Hz), 7.69 (1H, t, $J = 7.4$ Hz), 7.12 (1H, s), 5.53 (2H, s), 5.26 (2H, s), 4.55–4.27 (2H, m), 3.92 (2H, s), 3.42–3.26 (6H, m), 2.20–2.12 (2H, m), 0.94 (3H, t, $J = 7.1$ Hz), 0.89 ppm (3H, s); ^{13}C NMR (100 MHz, [D_6]DMSO): $\delta = 171.7$, 169.4, 167.1, 156.5, 152.3, 147.9, 146.1, 145.1, 131.5, 130.4, 129.8, 128.9, 128.5, 128.0, 127.7, 118.8, 94.9, 76.3, 73.9, 73.3, 68.2, 67.9, 66.3, 54.8, 50.2, 40.6, 30.2, 17.5, 7.5 ppm; IR (neat/NaCl): $\tilde{\nu} = 3400$, 2931, 2102, 1755, 1661, 1615, 1129 cm^{-1}; LRMS; (ESI): *m/z* $[MH]^+$ 592; HRMS (ESI): *m/z* $[MH]^+$ calcd for $C_{29}H_{29}N_5O_9$ 592.2038, found 592.2029; $[MNa]^+$ calcd for $C_{29}H_{29}N_5O_9Na$ 614.1857, found 614.1832.

CPT–linker-aminoPVA (3): A solution of **2** (21.1 mg, 0.0357 mmol), HOBt (4.8 mg, 0.0357 mmol) and EDC (13.7 mg, 0.0714 mmol) in DMF (714 μL, final concentration 0.05 M) was stirred for 60 min. A solution of aminoPVA in DMF/H_2O (1:1, 2.0 mL, 10 mg mL^{-1}, 2.5% N, *w/w*, 0.0357 mmol) was added and the reaction solution adjusted to pH ~6.5 with HCl (0.1 N) and/or NaOH (0.1 N) as needed. The mixture was stirred at RT for 1 day. After 16 h the solution was adjusted to the pH 6.5 if necessary. The solution was then dialyzed (Spectra/Por 6 dialysis membrane, MWCO 3500) against NaCl (0.2 N) for 3 days and then against H_2O for 2 days changing the solution twice daily. The dialyzed solution was further extracted multiple times with CH_2Cl_2 until TLC analysis (CH_2Cl_2/MeOH, 9:1) of the CH_2Cl_2 extracts was free of spots. Lyophilization of the crude material gave **3** as a white solid (3.7 mg).

Preparation of CPT–USPIO (4): Superparamagnetic iron oxide nanoparticles (ferrofluid) were prepared according to previously described methods.[29–31,33,34] Briefly, ferrofluid was prepared by alkaline co-precipitation of $FeCl_3$ (0.086 M) and $FeCl_2$ (0.043 M) (Fluka, Buchs, Switzerland). After washing with H_2O, the black precipitate was refluxed in nitric oxide (0.8 M)–$Fe(NO_3)_3 \cdot 9H_2O$ (0.21 M) (Fluka) for 1 h. The reaction was cooled and the brown precipitate dispersed in H_2O and dialyzed for 2 days against HNO_3 (0.01 M). This ferrofluid was mixed with PVA (3–83, Mowiol, 7600 g mol^{-1}, courtesy of Clariant) and aminoPVA (M12, Erkol, 20000 g mol^{-1}, courtesy of Erkol) as described previously[29,30] to obtain aminoPVA-USPIOs, and the pH was adjusted to 7.0. For the experiments described here, the ratio of total polymer to iron was 10 (mass ratios). As previously described,[30] for aminoPVA-USPIOs the mass ratio of PVA to aminoPVA copolymer was 45. For the preparation of CPT–USPIOs, the ferrofluid was mixed in ultrapure H_2O with PVA, aminoPVA copolymer and CPT–linker–aminoPVA **3** at defined ratios (Table 1), then the CPT–USPIOs **4** were stabilized at pH 6–7.

Physical characterization of CPT–USPIO 4

Particle sizes were measured by photon correlation spectroscopy (PCS) using a Brookhaven apparatus equipped with a BI-9000AT digital autocorrelator instrument and a He-Ne laser beam at a wavelength of 661 nm (scattering angle of 90°). The CONTIN method was used for data processing. Viscosity and refraction index of pure water were used for size distribution calculation. Coated-USPIOs were diluted 51 fold in 0.01 M HNO_3 in ultra pure water pre-filtered on 20 nm ceramic filters (Whatman, Anodisc 25). The same setting equipped with platinum electrodes was used for electrophoretic mobility measurements and ζ-potential was calculated using the Smoluchowski approximation. The electrodes were cleaned for 5 min in an ultrasonic bath prior to each measurement.

Gel filtration experiments

Samples of 15 μL of CPT–USPIOs were applied to a Sephadex G-75 column (0.6×19 cm, Pharmacia, Uppsala, Sweden) equilibrated in $NaH_2PO_4 \cdot 2H_2O$ (25 mM) and NaCl (0.15 M) at pH 7.0, prefiltered through a 0.22 μm filter (Millex GP, Millipore), at RT with a flow rate of 20 mL h^{-1}. The fractions were analyzed for Fe, PVA and fluorescence. For Fe determination, 50 μL of each fraction was mixed with HCl (50 μL, 6 N) for 1 h at RT and a solution of $K_4[Fe(CN)_6 \cdot 3H_2O]$ (100 μL, 5%) was added for 30 min. Absorbance was read at 690 nm in a multiwell plate reader (Labsystems iEMS Reader MF, BioConcepts, Allschwil, Switzerland) and Fe was quantified from a standard curve of aminoPVA-USPIOs treated under the same conditions. For PVA quantification, 110 μL of distilled water and 70 μL of a iodine solution (0.45% KI, 0.225% I_2 and 3.6% H_3BO_3 (*w/v*)) were added to 20 μL of each fraction and incubated at RT for 30 min. Absorbance was read at 690 nm in a multiwell plate reader and the amount of PVA was quantified from a standard curve of PVA treated under the same conditions. The fluorescence of CPT (in water) was measured at $\lambda_{ex}/\lambda_{em}$ of 360/460 nm in a multiwell plate reader (CytoFluor, Series 4000, PerSeptive Biosystems).

Cellular assays

Cells and cell treatment: The Me300 human melanoma cell line (donated by D. Rimoldi, Ludwig Institute, Lausanne, Switzerland) was grown in RPMI 1640 medium containing 10% fetal calf serum (FCS) and antibiotics (all from Gibco, Invitrogen, Basel, Switzerland) at 37 °C and 6% CO_2. Two to three days prior to experiments, the cells were detached with trypsin–EDTA (Gibco), centrifuged and grown in complete medium in 48-well or 96-well plates (Costar, Corning, NY, USA), in order to reach 60–80% confluence on the day of experiment. Fresh complete medium was added prior to exposure to the drugs for the concentration and time indicated. Stock solutions of (*S*)-(+)-CPT (Sigma–Aldrich, Buchs, Switzerland) in DMSO (20 mM) were prepared. DMSO at the same concentration was used as a control for CPT experiments. Experiments were performed in triplicate wells. [^{3}H]-Thymidine incorporation was measured to quantify DNA synthesis and Alamar Blue reduction was used to determine cell viability (see below). Alternatively, the cell layers were washed twice with saline and cellular iron content was quantified using the Prussian blue method and drug content by measuring drug fluorescence (see below).

Evaluation of cell viability and DNA synthesis: To quantify metabolically active cells, 10% Alamar blue (Serotec, Düsseldorf, Germany) was added to the cell culture medium and fluorescence increase was directly measured in a multiwell fluorescence reader ($\lambda_{ex}/\lambda_{em}$ = 530 nm/580 nm) after 2 h at 37 °C. To assess for DNA synthesis, 1 μCi mL^{-1} [^{3}H]-thymidine (Amersham Pharmacia, Dübendorf, Switzerland), was added for the last 2 h of exposure to compounds and incorporation was quantified in a beta-counter (Rackbeta, LKB) after precipitation with 10% trichloracetic acid and solubilization in 0.1 N NaOH and 1% sodium dodecylsulfate (SDS).

Total cell-bound iron and drug determination: The quantification of cell-associated nanoparticles was determined by cell iron content and histological determination of iron by Prussian blue reaction, performed as previously described.[30,31] Briefly, for quantitation of cell iron content, the cell layer was dissolved for 1 h in 6 N HCl (125 μL $well^{-1}$ of a 48-well plate), then 125 μL of a 5% solution of $K_4[Fe(CN)_6] \cdot 3H_2O$ in H_2O was added for 20 min and the absorbance was read at 690 nm in a multiwell plate reader. A standard curve of aminoPVA-USPIOs in 6 N HCl was treated in the same conditions to quantify the amount of cell-bound iron and the number of USPIOs added to or taken up by cells was calculated as previously described,[26] assuming a mean diameter of the iron oxide core of 9±3 nm. Cell-associated drug was determined in lysed cells by measuring fluorescence intensity in 0.1 N NaOH and 1% SDS at $\lambda_{ex}/\lambda_{em}$ of 360 nm/460 nm in a multiwell fluorescence plate reader. Histological determination of the cell-associated iron and CPT fluorescence in intact cells was performed on cells grown on histological slides. Following exposure to CPT–USPIOs **4**, the cell layers were extensively washed in PBS then slides were fixed in 100% cold EtOH for 10 min at 4 °C, dehydrated in graded alcohol to xylol and mounted. Samples were examined under a fluorescence microscope (Axioplan2, Carl Zeiss, AxioCam MRm camera, AxioVision Rel. 4.6 logiciel, Feldbach, Switzerland) and filter set at 365 nm excitation light (BP 365/12, FT 395, LP 397). Histological

cell-associated iron determination by Prussian blue reaction was performed as previously described.[30] Briefly, the cell layer was exposed for 15–30 min at RT to a 1:1 solution of 1 N HCl and 2.5% $K_4[Fe(CN)_6]$ in H_2O, washed with distilled water, counterstained with nuclear fast red, dehydrated in graded alcohol and mounted.

Histochemical determination of lipids and camptothecin: Cells were grown on histological slides then exposed to CPT–USPIO **4**. Cell layers were fixed in 70% alcohol and exposed for 2 min to a Sudan solution (water/EtOH/acetone, 3:7:10; 0.7% (*w*/*v*) Sudan III (Fluka, Buchs, Switzerland), 0.7% (*w*/*v*) Sudan IV (BDH Chemicals Ltd., Poole, England), sequentially washed in 70% alcohol, tap water, and counterstained with hematoxylin, then mounted in an aqueous mounting medium (Immu-mount, Thermo Scientific, Pittsburgh, USA). Slides were photographed under a Nikon digital camera (DXM 1200; Nikon Corporation, Tokyo, Japan).

Enzymatic digestion of CPT–USPIOs 4 and evaluation of drug release: The release of CPT from CPT–USPIO conjugate **4** was evaluated by harvesting confluent layers of human Me300 melanoma cells. The cells were scraped from the plates and extracted with phosphate/NaCl buffer (pH 7.4) by three cycles of freeze-thaw in liquid nitrogen. Two volumes of CPT–USPIO **4** were exposed for 24 h at 37 °C to one volume of cell extract, centrifuged for 5 min at 1000 rpm, and the supernatant (20 μL) was applied to a Sephadex G-75 column in phosphate buffer (pH 7), and the eluting fractions were monitored for iron, PVA and CPT.

Transmission electron microscopy: Me300 cells were grown in complete medium in a 25 cm^2 flask (Nunclon, from Milian, Geneva, Switzerland) in order to reach 70–80% confluence on the day of experiment. Fresh complete medium was added prior to exposure to CPT–USPIOs **4** for the concentration and time indicated. Cells were washed twice with PBS and 1 mL trypsin/versene (Gibco) was added for 5 min at 37 °C. Cells were centrifuged (5 min, 1000 rpm) and the supernatant was removed. The cell pellet was fixed in 2% glutaraldehyde buffered in 0.05 M cacodylate and centrifuged. Cells were kept in fixative solution for 48 h, then washed three times with 0.2 M cacodylate, postfixed in 1.3% osmium tetroxide in 0.2 M cacodylate for 1 h and dehydrated in graded EtOH, then propylene oxide. Cell pellets were embedded in epon (50% (*w*/*w*) epon 812 substitute, 26% (*w*/*w*) dodecenylsuccinic anhydride (DDSA), 23% (*w*/*w*) methylnadic anhydride (MNA), 1% (*w*/*w*) 2,4,6-tris(dimethylaminomethyl)phenol (DMP-30)). All reagents were purchased from Fluka. Blocks were cured for 48 h at 60 °C, thin sections (50 nm) were cut using an ultramicrotome (Ultracut E, Reichert-Jung Optische Werke AG, Wien, Austria) and mounted on 3 mm 200-mesh copper grids. Grids were stained using a standard two-step uranyl acetate/lead citrate (Fluka and Lavrylab, Saint-Fons, France) technique (Leica EM Stain) and then examined and photographed at 80 kV with a Philips CM10 transmission electron microscope combined with a MegaView III, Soft Imaging system. Elemental analysis of iron was performed using an electron Detection X-ray (EDAX, EDX-4), coupled to the CM12 transmission electron microscope.

Magnetic activation of CPT–USPIOs 4: The cells were detached with trypsin/versene (Gibco), centrifuged and grown in complete medium in 48-well plates (Costar) excluding the external wells of the plate, in order to reach 60–80% confluence on the day of experiment. Fresh complete medium was added prior to exposure to the drugs for the concentration and time indicated at 37 °C and 6% CO_2 without or with exposure to a static magnetic field. The magnetic field exposure was obtained by incubating the cells in the cell culture incubator onto 48 magnets inserted into the wells of a 48-well plate. Cylindrical (10 mm diameter, 5 mm height) NdFeB/N35 neodymium-boron-iron permanent magnets, magnetized axially and coated with Ni (Maurer Magnetic, Gröningen, Switzerland) were used (remanence, $B_r = 1.2$ T). Under this experimental setting, the cell layer is located ~2 mm from the magnets and the upper layer of the culture medium containing the CPT–USPIOs is located 6 mm away from the magnet. At the level of cells (~2 mm from the surface of the magnets) a magnetic flux density of 265 mT and a field gradient of 72 $T m^{-1}$ was induced (calculated using vizimag 3.5, http://www.vizimag.com). In order to obtain almost identical magnetic field conditions, the external wells of the cell plate were not used. After the incubation period, the cell layers were treated as above.

Calculation of results: Each experiment was repeated in triplicate wells at least twice. Means and standard deviation were calculated.

Acknowledgements

We would like to thank Mrs. Catherine Chapuis Bernasconi for excellent technical assistance. This work was supported by grants from the Swiss National Scientific Research Foundation (grant number 3152A0-105705) and the Swiss League and Research against Cancer (grant number KLS-01308-02-2003). We also thank NSERC (Canada) and FQRNT (Province of Quebec) for financial assistance. We would specifically like to thank and dedicate this paper to Auxia Montoro who developed the TEM techniques necessary to this work, and became very ill at the very end of this project.

Keywords: antitumor agents · chemical functionalization · drug delivery · nanoparticles · superparamagnetism

[1] J. S. Ross, D. P. Schenkein, R. Pietrusko, M. Rolfe, G. P. Linette, J. Stec, N. E. Stagliano, G. S. Ginsburg, W. F. Symmans, L. Pusztai, G. N. Hortobagyi, *Am. J. Clin. Pathol.* **2004**, *122*, 598–609.
[2] R. Haag, F. Kratz, *Angew. Chem.* **2006**, *118*, 1218–1237; *Angew. Chem. Int. Ed. Engl.* **2006**, *45*, 1198–1215.
[3] I. Brigger, C. Dubernet, P. Couvreur, *Adv. Drug Delivery Rev.* **2002**, *54*, 631–651.
[4] L. Juillerat-Jeanneret, F. Schmitt, *Med. Res. Rev.* **2007**, *27*, 574–590.
[5] S. Parveen, S. K. Sahoo, *J. Drug Targeting* **2008**, *16*, 108–123.
[6] K. Cho, X. Wang, S. Nie, Z. Chen, D. M. Shin, *Clin. Cancer Res.* **2008**, *14*, 1310–1316.
[7] L. Juillerat-Jeanneret in *Nanotechnologies for the Life Sciences, Vol. 6* (Ed.: C. S. S. R. Kumar), Wiley-VCH, Weinheim, **2006**, pp. 199–232.
[8] L. D. Galuppo, S. W. Kamau, B. Steitz, P. O. Hassa, M. Hilbe, L. Vaughan, S. Koch, A. Fink-Petri, M. Hofman, H. Hofman, M. O. Hottiger, B. von Rechenberg, *J. Nanosci. Nanotechnol.* **2006**, *6*, 2841–2852.
[9] G. F. Goya, V. Grazú, M. R. Ibarra, *Curr. Nanosci.* **2008**, *4*, 1–16.
[10] M. Arruebo, R. Fernández-Pacheco, M. R. Ibarra, J. Santamaria, *Nano Today* **2007**, *2*, 22–32.
[11] A. K. Gupta, M. Gupta, *Biomaterials* **2005**, *26*, 3995–4021.
[12] T. Neuberger, B. Schöpf, H. Hofmann, M. Hofmann, B. von Rechenberg, *J. Magn. Magn. Mater.* **2005**, *293*, 483–496.
[13] R. G. Schoenmakers, P. van de Wetering, D. L. Elbert, J. A. Hubbell, *J. Controlled Release* **2004**, *95*, 291–300.
[14] C. Alexiou, W. Arnold, R. J. Klein, F. G. Parak, P. Hulin, C. Bergemann, W. Erhardt, S. Wagenpfeil, A. S. Lübbe, *Cancer Res.* **2000**, *60*, 6641–6648.
[15] C. Alexiou, R. Jurgons, R. J. Schmid, C. Bergemann, J. Henke, W. Erhardt, E. Huenges, F. Parak, *J. Drug Targeting* **2003**, *11*, 139–149.
[16] T. K. Jain, M. A. Morales, S. K. Sahoo, D. L. Leslie-Pelecky, V. Labhasetwar, *Mol. Pharm.* **2005**, *2*, 194–205.

[17] N. Nasongkla, E. Bey, J. Ren, H. Ai, C. Khemtong, J. S. Guthi, S.-F. Chin, A. D. Sherry, D. A. Boothman, J. Gao, *Nano Lett.* **2006**, *6*, 2427–2430.
[18] A. S. Lübbe, C. Bergemann, W. Huhnt, T. Fricke, H. Riess, J. W. Brock, D. Huhn, *Cancer Res.* **1996**, *56*, 4694–4701.
[19] S. Rudge, C. Peterson, C. Vessely, J. Koda, S. Stevens, L. Catterall, *J. Controlled Release* **2001**, *74*, 335–340.
[20] R. Weissleder, K. Kelly, E. Y. Sun, T. Shtatland, L. Josephson, *Nat. Biotechnol.* **2005**, *23*, 1418–1423.
[21] D. Devineni, C. D. Blanton, J. M. Gallo, *Bioconjugate Chem.* **1995**, *6*, 203–210.
[22] N. Kohler, C. Sun, J. Wang, M. Zhang, *Langmuir* **2005**, *21*, 8858–8864.
[23] N. Kohler, C. Sun, A. Fichtenholtz, J. Gunn, C. Fang, M. Zhang, *Small* **2006**, *2*, 785–792.
[24] Y. Pommier, *Nat. Rev. Cancer* **2006**, *6*, 789–802.
[25] H. Ulukan, P. W. Swaan, *Drugs* **2002**, *62*, 2039–2057.
[26] P. Pantazis, H. R. Hinz, J. T. Mendoza, A. J. Kozielski, L. J. Williams, Jr., J. S. Stehlin, Jr., B. C. Giovanella, *Cancer Res.* **1992**, *52*, 3980–3987.
[27] M. Watanabe, K. Kawano, M. Yokoyama, P. Opanasopit, T. Okano, Y. Maitani, *Int. J. Pharm.* **2006**, *308*, 183–189.
[28] J. Williams, R. Lansdown, R. Sweitzer, M. Romanowski, R. LaBell, R. Ramaswami, E. Unger, *J. Controlled Release* **2003**, *91*, 167–172.
[29] M. Chastellain, A. Petri, H. Hofmann, *J. Colloid Interface Sci.* **2004**, *278*, 353–360.
[30] A. Petri-Fink, M. Chastellain, L. Juillerat-Jeanneret, A. Ferrari, H. Hofmann, *Biomaterials* **2005**, *26*, 2685–2694.
[31] F. Cengelli, D. Maysinger, F. Tschudi-Monnet, X. Montet, C. Corot, A. Petri-Fink, H. Hofmann, L. Juillerat-Jeanneret, *J. Pharmacol. Exp. Ther.* **2006**, *318*, 108–116.
[32] S. Hanessian, J. A. Grzyb, F. Cengelli, L. Juillerat-Jeanneret, *Bioorg. Med. Chem.* **2008**, *16*, 2921–2931.
[33] R. Massart, E. Dubois, V. Cabuil, E. Hasmonay, *J. Magn. Magn. Mater.* **1995**, *149*, 1–5.
[34] G. A. van Ewijk, G. J. Vroege, A. P. Philipse, *J. Magn. Magn. Mater.* **1999**, *201*, 31–33.

Received: December 11, 2008
Revised: March 2, 2009
Published online on April 3, 2009

